Fuel 88 (2009) 988–993

Contents lists available at ScienceDirect

Fuel

journal homepage: www.elsevier.com/locate/fuel

In situ high-temperature phase transformation studies on pyrite

S.K. Bhargava *, A. Garg, N.D. Subasinghe

School of Applied Sciences, Applied Chemistry, RMIT University, GPO Box 2476V, Melbourne, VIC 3001, Australia

ARTICLE INFO

Article history:
Received 7 October 2008
Received in revised form 8 December 2008
Accepted 9 December 2008
Available online 4 January 2009

Keywords:
Oil shale
Pyrite
Phase transformations

ABSTRACT

Oil shales and coal have considerable amount of pyrite which undergoes various thermal transformations during their processing or combustion. Reactions and changes in pyrite chemistry vary considerably under different environmental conditions. In this paper, we report an *in situ* high-temperature X-ray diffraction study of phase transformations in pyrite under variable environmental conditions (atmospheric pressure (1 atm.), low air pressure (<0.001 atm.), inert and carbon dioxide atmosphere). We observe that while heating of pyrite in air promotes the formation of hematite (α-Fe_2O_3), magnetite (Fe_3O_4) is a major product in low pressure environment. On the other hand, in the inert environments (nitrogen and argon) pyrrhotite, a non-stoichiometric iron sulphide, is the most dominant product. However, in carbon dioxide (CO_2) environment, pyrrhotite is an intermediate low temperature product which further transforms into magnetite and hematite, attributed to the dissociation of the CO_2 into O_2 and CO providing conducive conditions for the oxidation. We also propose the possible reaction pathways including self-dissociation of CO_2.

© 2008 Elsevier Ltd. All rights reserved.

1. Introduction

In countries such as Australia, use of pyrite containing fuel such as coal and oil shale poses major environmental concerns as energy sources [1,2]. Pyrite, with chemical formula FeS_2 contains large amounts of sulphur in addition to many other trace elements such as Co, Ni, Cu, Mo etc. [3,4]. During processing of oil shales, pyrite undergoes a number of chemical reactions and these reactions are affected by the nature of processing environment. Industrially important processes are retorting processes involving heating oil shales to temperatures above 550 °C in low-oxygen atmosphere or combustion of coal or oil shales in the form of direct fuel which is conducted under standard atmospheric conditions. These reactions are important due to several factors. For instance, in natural environments, oxidation of pyrite may generate sulphuric acid, which can either alter other minerals or can lower the pH of the surrounding environment. On the other hand, in industrial applications such as oil shale retorting and coal combustion, pyrite may decompose to release corrosive gases such as SO_2 or SO_3 [3–6].

Previous studies on the thermal decomposition and reactions of pyrite suggest that the products of decomposition vary depending upon the environment. For instance, it is easily oxidised to different iron oxides such as hematite (α-Fe_2O_3) or magnetite (Fe_3O_4) in an oxidizing environment [7], while pyrrhotite is one of the major products of pyrite decomposition in non-oxidative environments [8]. Other products may also be formed in different gaseous environments.

Eneroth and Koch [9] studied the thermal oxidation of pyrite and its polymorph, marcasite by heating pyrite between 200 and 650 °C for 1 h in the presence of oxygen and reported hematite as the main product. There are various reports on the transformation of pyrite into hematite: some suggesting direct transformation of pyrite into hematite upon heating in air [10] while others show transformation into hematite via intermediate stage of pyrrhotite formation [11]. The different mechanisms of pyrite to hematite transformation in oxidizing environments proposed by different groups are governed by factors such as particle size, temperature, oxygen concentration, heating rate and flow conditions [7]: for instance lower temperature (<800 K) and oxygen-rich environments lead to direct oxidation of pyrite whereas higher temperature (>800 K) and low-oxygen containing atmospheres give rise to oxidation via intermediate formation of pyrrhotite. While in most cases, hematite is the commonly reported final product, there are occurrences of magnetite formation if the oxygen concentration of the environment is relatively low (1–5%), especially at higher temperatures (typically higher than 1273 K) [12–15].

In non-oxidizing environments, pyrite transforms into pyrrhotite (a non-stoichiometric Fe sulphide with the general formula $Fe_{1-x}S$, where $x \leqslant 0.125$) via reaction (1)

$$FeS_2 + 2CO_2 \rightarrow Fe_{1-x}S + 2CO(g) + SO_2(g) \quad (1)$$

Mechanical milling of pyrite in carbon dioxide (CO_2) has been shown to transform pyrite into monoclinic pyrrhotite and further milling converted the monoclinic pyrrhotite into hexagonal

---

* Corresponding author.
E-mail address: suresh.bhargava@rmit.edu.au (S.K. Bhargava).

0016-2361/$ - see front matter © 2008 Elsevier Ltd. All rights reserved.
doi:10.1016/j.fuel.2008.12.005

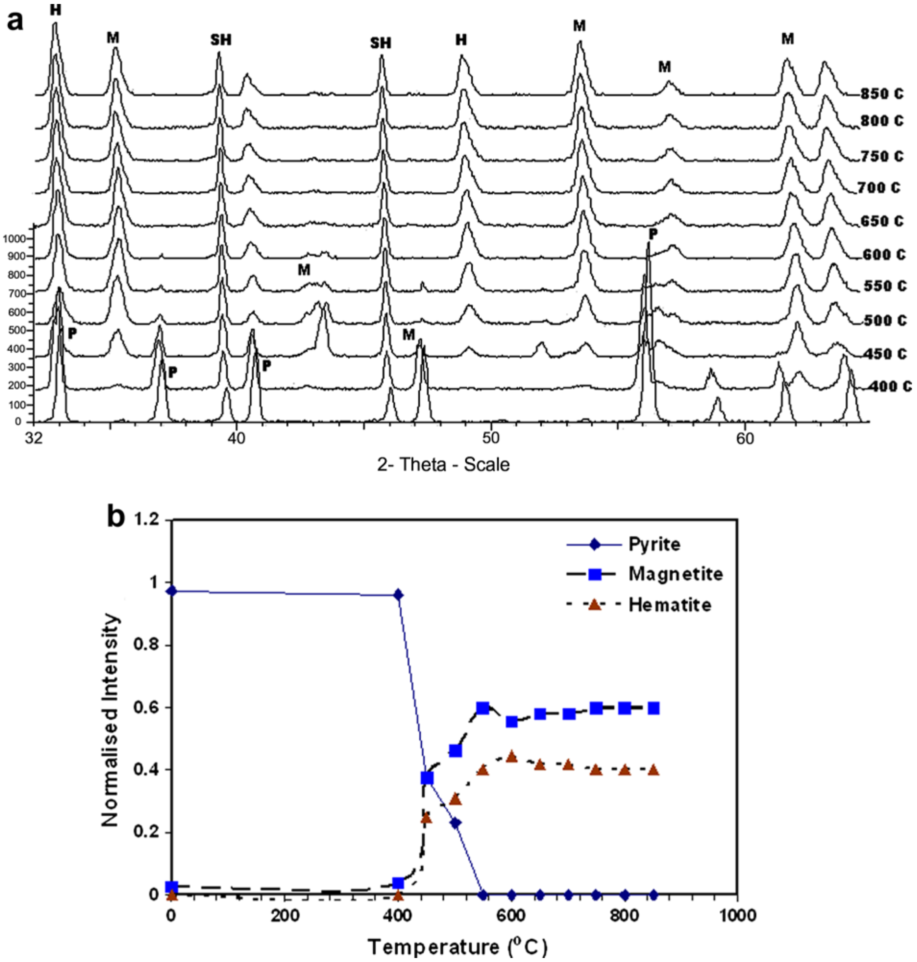

Fig. 1. (a) *In situ* HTXRD patterns of pyrite analysed under low pressure (<0.001 atm.). Bottom unlabelled pattern is of pyrite at room temperature; P – pyrite, Pyrh – pyrrhotite, H – hematite, M – magnetite, SH – sample holder. (b) Normalised intensities as a function of temperature.

pyrrhotite, with a sulphur deficiency which was attributed to the formation of amorphous sulphur [16]. Authors also argued that pyrrhotite is stable in CO_2 environments. It has also been reported that the reactions of pyrite and CO_2 involve the breakdown of sulphide via an exothermic reaction [17,18]. Subasinghe et al. [19] studied the reactions of minerals in oil shale in different gaseous environments and showed that pyrite disappears much faster in air than in a non-oxidizing environment.

Previous studies on Venus' atmosphere revealed the presence of reduced sulphur gases [17,18] that led to a few studies on pyrite decomposition and formation of carbonyl sulphide (OCS) and sulphur in CO_2, CO and SO_2 atmospheres at high-temperatures. Hong and Fegley [18] investigated the possibilities of the following reactions towards the formation of OCS:

$$SO_2 + 3CO \Rightarrow OCS + 2CO_2 \tag{2}$$

$$3FeS_2 + 4CO_2 + 2CO \Rightarrow Fe_3O_4 + 6OCS \tag{3}$$

$$2CO + S_2 \Rightarrow 2OCS \tag{4}$$

Hong and Fegley [18] observed that OCS gas was produced when pyrite was heated at relatively higher temperatures (538–612 °C). They also suggested that OCS might have been formed by reactions (2) and (4) rather than (3).

Whilst previous literature reports have led to an enhanced understanding of the reactions and detailed reaction mechanisms of transformations of pyrite, there are disagreements between various groups [7–16]. This could be because most of the previously conducted studies were *ex situ*, *i.e.* on heated and quenched/cooled products, at times not revealing the complete process of the transformation by hindering access to intermediate transformation products. The objective of this paper is to study the transformation of pyrite using an *in situ* high-temperature X-ray diffraction (XRD) in different environments and to analyse the process of transformation while being able to compare and contrast with previously reported results. It is also hoped that this study would also shed more light into environmental aspects of fuel processing.

2. Experimental

2.1. Material and methods

Natural pyrite samples from South Australia were used for all analyses. The samples were crushed immediately before use, to a grain size between 75 and 125 μm under ethanol to avoid possible oxidation reactions beforehand. The samples were not ground to a fine powder in order to prevent any strain and to reduce possible reactions during grinding. After preliminary XRD and XRF analysis and semi-quantification, only samples with the minimum level of impurities were selected for further studies.

2.2. XRF analyses

Quantitative analysis of major and minor elements was carried out using a Bruker S4 Pioneer wavelength dispersive X-ray fluores-

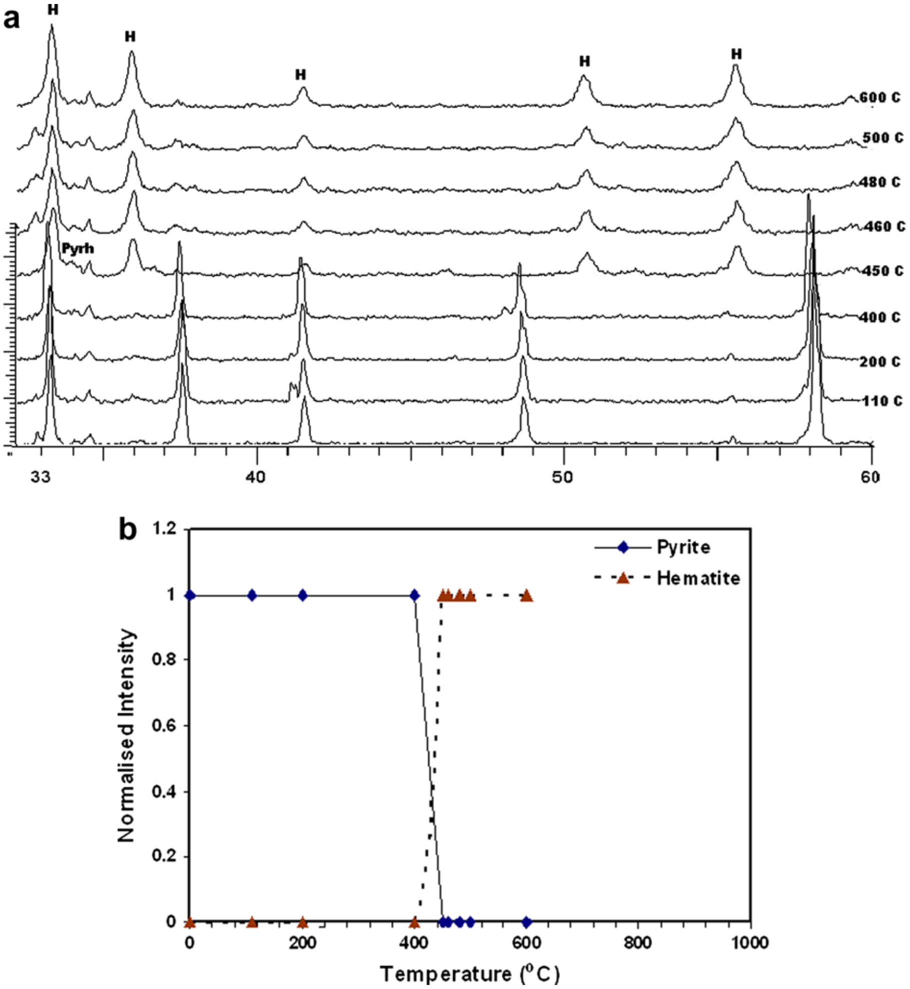

Fig. 2. (a) *In situ* HTXRD patterns of pyrite analysed in air (atmospheric pressure). Bottom trace is of pyrite at room temperature; Pyrh – pyrrhotite, H – hematite. (b) Normalised intensities as a function of temperature.

cence spectrometer, operated using a 4 kW tube at 50 kV and 40 mA. The selected pyrite sample showed an average of 45.27% w/w iron and 52.82% w/w sulphur, which is characteristic of 98.1% pure pyrite with minute amounts of Si (0.67%), Ca (0.27%), Zn (0.16%), Al (0.14%), and traces of Pb and As (<0.1%). These values are comparable to most of the natural samples used by other researchers [20].

2.3. In situ HTXRD

X-ray diffraction analyses were run on a Bruker XRD diffractometer using Cu Kα radiation in θ–2θ coupled mode with 0.01 degree step size and 2 s/step sampling time. To conduct the measurements, each powder sample was placed directly on the platinum heating strip. The samples were heated to various temperatures a heating rate of 10 °C/min and were held at various temperatures for 2 min before recording the spectra. Peaks from the platinum sample holder were also visible in some diffractograms and were labelled accordingly. The measurements were made in air, under low vacuum (<0.001 atm.), argon, nitrogen and carbon dioxide, respectively. The gas flow rates were maintained at 20 ml/min in all the appropriate experiments. The gases were bled in to the chamber for a minimum of 30 min prior each analysis to attain steady state conditions.

There was a minor shift in XRD peaks at high-temperatures due to thermal expansion of the sample and the platinum sample holder and was taken into account while identifying the peaks.

3. Results and discussion

Room temperature XRD results of the pyrite sample match with the JCPDS file no. 71-2219, for cubic pyrite with *a* = 5.4179 Å. Pyrite is known to decompose and undergo various transformation above 400 °C [9,17,18,21,22] and thus all the XRD measurements were performed at temperatures up to 900 °C and the results are presented at and above 400 °C when no changes were found below 400 °C. Following sections present the *in situ* XRD results of the pyrite samples studied in different kinds of atmospheres.

3.1. Under low pressure (<0.001 atm.)

Fig. 1a shows the XRD patterns of the pyrite samples heated and measured at temperatures above 400 °C and up to 850 °C. No significant phase changes in the pyrite composition were observed at temperatures below 400 °C and the results are in accordance with the observations made by Hu et al. [22]. Although pyrite can potentially decompose below 400 °C [22], the reaction is very slow and no significant changes were observed from the experiments and subsequent XRD patterns of the samples. However, as the temperature reaches 400 °C, one could observe the appearance of magnetite peaks followed by appearance of hematite peaks at 450 °C. Upon further heating the sample, pyrite peaks disappear at about 600 °C and at further higher temperatures, a mixture of magnetite and hematite coexists. This is also depicted in Fig. 1b which shows the variation in the normalized relative intensity of the strongest peak of each phase with temperature, clearly indicating the change in the amounts of different phases with temperature.

As depicted in Fig. 1a and b, in the low pressure environment, pyrite produces magnetite as the major product, through an intermediate phase of pyrrhotite (pyrite → pyrrhotite → magnetite and hematite). Eventually magnetite is slowly converted into hematite. This is an expected outcome under such restrictive oxidation conditions prevailing in low air pressure [7].

3.2. In air

Fig. 2a shows that *in situ* HTXRD traces of pyrite heated and held at various temperatures up to 900 °C. The figure shows that while only pyrite peaks are seen until 400 °C, formation of hematite with disappearance of pyrite peaks is noted at and above 450 °C. No other form of iron oxide is seen to form suggesting presence of high enough oxygen concentration in the environment and confirming the results of researchers reporting direct decomposition of pyrite in to hematite [7].

Reactions of Pyrite with oxygen to produce hematite (Fe_2O_3) and magnetite (Fe_3O_4) are represented as follows [23–25]:

$$2FeS_2 + 51/2O_2 \rightarrow Fe_2O_3 + 4SO_2(g) \qquad (5)$$

$$3FeS_2 + 8O_2 \rightarrow Fe_3O_4 + 6SO_2(g) \qquad (6)$$

Above observations are also shown graphically in Fig. 2b where normalized relative intensities of strongest peaks of both pyrite and hematite are plotted as a function of temperature and once could again observe a sharp change in the intensities of both peaks confirming the phase change.

3.3. In Argon and nitrogen

Fig. 3a and b shows the XRD patterns of the samples when heated and held at various temperatures up to 900 °C. In this case, there is a sharp change in the pattern at 600 °C which suggests the phase change between 550 and 600 °C as at 500 °C, sample still consisted of pyrite phase. This shows that pyrite decomposition in argon does not start until about 550–600 °C unlike air where transformation starts below 500 °C (see Section 3.2. and Fig. 2a). In inert atmospheres, the final product is pyrrhotite, non-stoichiometric iron sulphide as against formation of hematite in air, reflecting the role of oxygen played in final phase formation. Pyrrhotite remains stable even at higher temperatures when heated up to 900 °C as shown by the XRD patterns. The peak-to-noise ratio is lower for the XRD patterns recorded in argon because of argon's higher X-ray scattering cross-section and mass absorption coefficient. The change in the normalized relative intensities of the strongest peaks of two phases, as shown in Fig. 3b is also indicative of the above change.

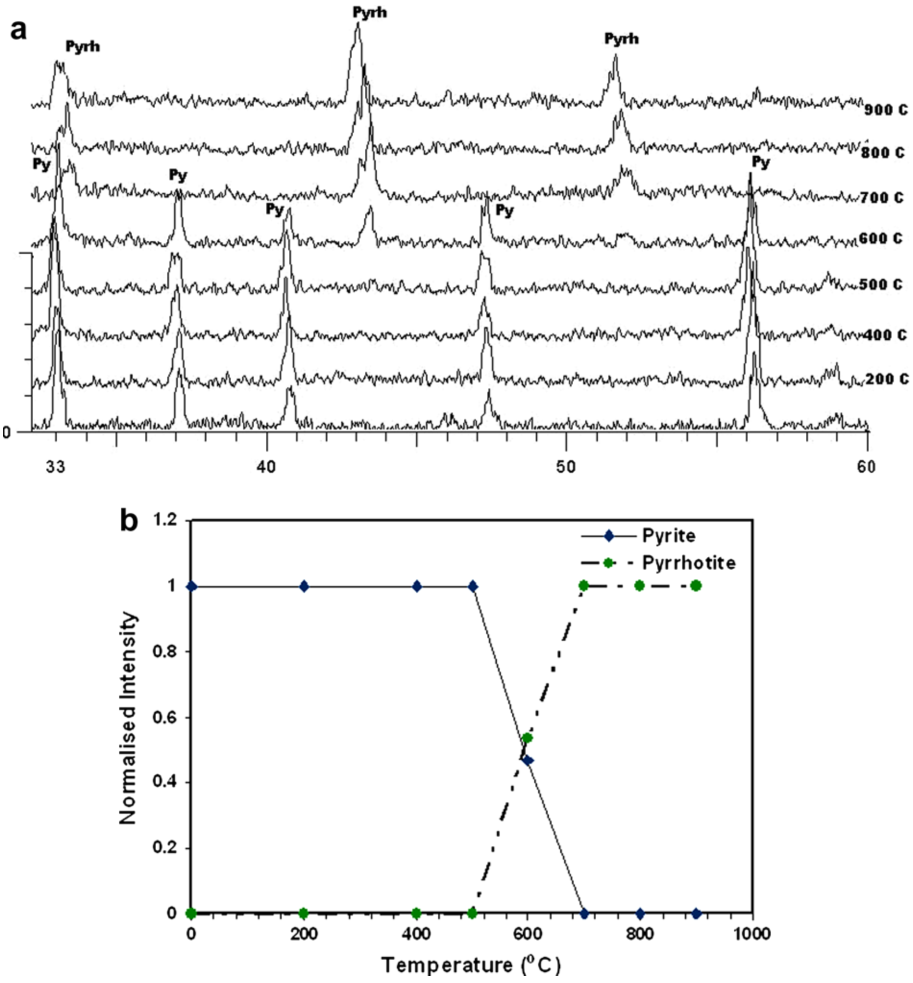

Fig. 3. (a) *In situ* HTXRD patterns of pyrite analysed in argon. Bottom trace is of pyrite at room temperature; Py – pyrite, Pyrh – pyrrhotite. (b) Normalised intensities as a function of temperature.

Transformation of pyrite to pyrrhotite is shown by the following reaction [8]:

$$\mathrm{Fes_2} \leftrightarrow \mathrm{FeS}_x(\mathrm{s}) + (1 - 0.5x)\mathrm{S_2(g)} \tag{7}$$

which is an endothermic process and this explains the reason for pyrite to pyrrhotite transformation requiring higher temperature than pyrite to hematite transformation [26].

For samples measured in pure nitrogen atmosphere, a similar trend to that in argon was observed thus the XRD traces are not shown here. However, in our early experiments with impure N_2, we observed the presence of small amounts of magnetite at higher temperatures which could have arisen due to small amounts of oxygen and/or water vapour in the nitrogen gas. Hurst et al. [21] reported that just 1.2% of oxygen in a nitrogen atmosphere can oxidise pyrite to FeO and Fe_3O_4 via an intermediate step of pyrrhotite formation. Complete removal of oxygen and water vapour from nitrogen prevents the formation of the oxides, with the reaction terminating upon pyrrhotite formation.

3.4. In carbon dioxide (CO_2)

Fig. 4a shows the *in situ* XRD patterns of the pyrite sample treated and measured in CO_2 atmosphere. The results suggest that initially, from 500 °C onwards, pyrite starts converting to pyrrhotite and at 600 °C, only pyrrhotite is seen. This is also corroborated by Fig. 4b where pyrite peak intensity drops to zero where as pyrrhotite peak intensity is 100% at 600 °C. However, pyrrhotite remains stable only below 800 °C. Heating the sample at 800 °C and above leads to the formation of magnetite and smaller amounts of hematite.

Aylmore and Lincoln [23,24] extensively studied the reactions of pyrite, arsenopyrite and pyrrhotite in CO_2 and suggested that the presence of CO_2 may increase the rate of partial breakdown of pyrite and produce pyrrhotite according to reactions (8)–(11)

$$\mathrm{FeS_2 + 2CO_2(g) \leftrightarrow Fe_{1-x}S + 2CO(g) + SO_2(g)} \tag{8}$$

$$\mathrm{7FeS_2 + 2SO_2(g) \rightarrow Fe_7S_8 + 2O2(g) + 8S} \tag{9}$$

$$\mathrm{Fe_7S_8 + 2SO_2(g) + 4S \rightarrow 7FeS_2 + 2O_2(g)} \tag{10}$$

$$\mathrm{24FeS_2 + 7SO_2(g) \rightarrow 2Fe_7S_8 + 2Fe_3O_4 + 2Fe_2O_3 + 39S} \tag{11}$$

Among these, reaction (9) is the most likely reaction because with continuous purging of CO_2 gas, it is highly unlikely that SO_2 builds up to sufficient concentration to react with pyrite as in Eqs. (9)–(11). This also explains the absence of sulphur as a by-product.

In general, as the literature suggests, at high-temperatures (1173–1273 K) and high enough oxygen concentrations, all the pyrite oxidation reactions preferentially form a higher oxidation product, namely hematite as studied using techniques such as X-ray diffraction [7,9,27,28]. Under such conditions, nearly all of the iron present in the samples converts into highest oxidation state of Fe *i.e.* Fe^{3+}, present in the form of hematite. On the other hand, magnetite, a mixed valence oxide, is seen to form at higher temperatures and/or at lower oxygen concentrations where sufficient oxygen is not present to yield complete oxidation of iron to

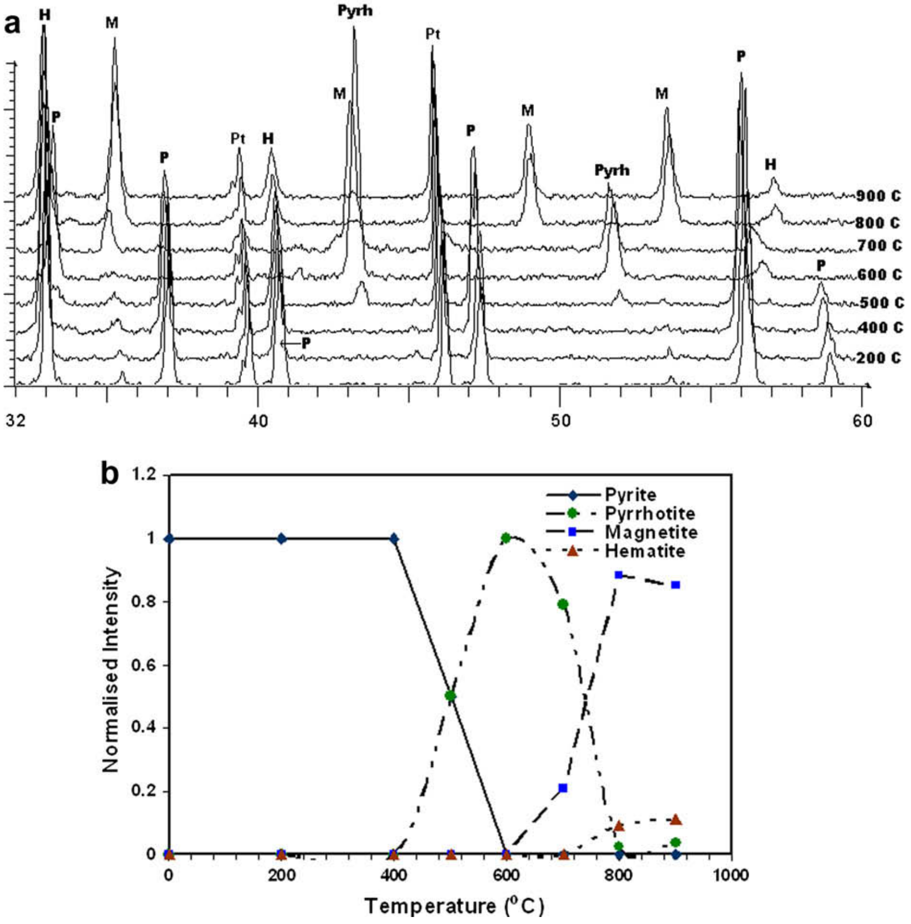

Fig. 4. (a) *In situ* HTXRD patterns of pyrite analysed in CO_2. Bottom trace is of pyrite at room temperature. Two unmarked peaks around 39.5 and 46.2° 2θ are for the platinum sample holder; H – hematite, M – magnetite, P – pyrite, Pyrh – pyrrhotite. (b) Normalised intensities as a function of temperature.

achieve the highest oxidation state [7]. On the other hand in CO_2, at low enough temperatures, pyrite undergoes thermal decompositions to yield pyrrhotite, though presence of small amounts of oxygen may promote the oxide formation [26].

In CO_2, formation of magnetite and smaller amounts of hematite at higher temperatures, as shown in Fig. 4, can be attributed to the instability of CO_2 and its dissociation into CO and O_2, there by leading to oxidation of pyrrhotite. This was also shown by Fegley et al. [17] who measured the oxygen fugacity in CO_2 before and after heating to 500 °C and showed self-dissociation of CO_2 into CO and O_2. The researchers further reported the formation of hematite (α-Fe_2O_3) and maghemite (γ-Fe_2O_3) mixture from magnetite in CO/CO_2 gas. In our experiments, CO_2 dissociation above 700 °C provides a gaseous atmosphere similar to that described by Fegley et al. [17]. As indicated in Fig. 4, pyrrhotite is an intermediate phase produced during heating of pyrite. In a restrictive oxidative environment, magnetite is the major reaction product along with small amounts of hematite.

Considering the above factors, the following reactions are proposed for the decomposition of pyrite in CO_2 gas:

$$FeS_2 + 2CO_2(g) \rightarrow Fe_{1-x}S + 2CO(g) + SO_2(g) \tag{12}$$

$$Fe_{1-x}S + CO(g) \rightarrow Fe_3O_4 + COS(g) + SO_2(g) \tag{13}$$

The overall reaction is

$$FeS_2 + CO_2(g) \rightarrow Fe_3O_4 + Fe_2O_3 + COS(g) + SO_2(g) \tag{14}$$

No evidence of sulphur was observed during this work, although small amounts of amorphous sulphur could potentially form. Using the available data, the reaction path above (reaction (14)) is considered most suitable.

4. Summary

We have conducted an *in situ* XRD study to investigate the phase transformation in natural pyrite under different environmental conditions namely air, low vacuum (<0.001 atm.), inert gases (nitrogen and argon) and CO_2 atmospheres using a high-temperature X-ray diffractometer. The end reaction product and the sequence of phase formation varied depending on the reaction environment. While in air, pyrite directly transformed to hematite as the only reaction product, in restrictive oxidating environment such as vacuum, magnetite and hematite were found to coexist. In the inert atmospheres such as argon and nitrogen, pyrite simply converts to pyrrhotite as the end product with transformation occurring at relatively higher temperatures than in air and is attributed to the endothermic reaction of transformation. In CO_2, it was observed that pyrite first reacts with CO_2 to form pyrrhotite near 500 °C which further decomposes near 800 °C into magnetite and small amounts of hematite. Latter is attributed to the dissociation of CO_2 into CO and O_2 at higher temperatures providing an oxidizing environment conducive towards formation of magnetite and hematite. This study on *in situ* identification of various phases upon pyrite decomposition could be useful for the industrial processes involving coal and oil shale such as retorting and combustion.

Acknowledgements

The authors thank the Australian Research Council for their financial assistance and the School of Applied Sciences (Applied Chemistry), RMIT University for use of HTXRD and XRD facilities.

References

[1] Patterson JH, Dale LS, Fardy JJ, Ramsden AR. Characterization of trace elements in rundle and condor oil shales. Fuel 1987;66:319–22.

[2] Swaine DJ, Goodarzi F. Environmental aspect of trace elements in coal. 1st ed. Springer; 1995.

[3] Subasinghe ND, Awaja F, Bhargava SK. Variation of kerogen content and mineralogy in some Australian tertiary oil shales. Fuel 2009;88:335–9.

[4] Abraitis PK, Pattrick RAD, Vaughan DJ. Variations in the compositional, textural and electrical properties of natural pyrite: a review. Int J Miner Process 2004;74:41–59.

[5] Levy JH, White TJ. The reaction of pyrite with water vapour. Fuel 1998;67:1336–9.

[6] Patterson JH, Hurst HJ, Levy JH, Killingley JS. Mineral reactions in the processing of Australian tertiary oil shales. Fuel 1990;69:1119–23.

[7] Hu G, Dam-Johansen K, Wedel S, Hansen JP. Decomposition and oxidation of pyrite. Prog Energ Combust Sci 2006;32:295–314.

[8] Toulmin P, Barton PB. A thermodynamic study of pyrite and pyrrhotite. Geochim Cosmochim Acta 1964;28:641–71.

[9] Eneroth E, Koch CB. Crystallite size of haematite from thermal oxidation of pyrite and marcasite – effects of grain size and iron disulphide polymorph. Miner Eng 2003;16:1257–67.

[10] Schorr JR, Everhart JO. Thermal behavior of pyrite and its relation to carbon and sulfur oxidation in clays. J Am Ceram Soc 1969;52:351–4.

[11] Jorgensen FRA, Moyle FJ. Phases formed during the thermal analysis of pyrite in air. J Therm Anal 1982;25:473–85.

[12] Prasad A, Singru RM, Biswas AK. Study of the roasting of pyrite minerals by Mössbauer spectroscopy. Phys Status Solidi A 1985;87:267–71.

[13] Srinivasachar S, Helble JJ, Boni AA. Mineral behavior during coal combustion 1. Pyrite transformations. Prog Energ Combust Sci 1990;16:281–92.

[14] McLennan AR, Bryant GW, Stanmore BR, Wall TF. Ash formation mechanisms during pf combustion in reducing conditions. Energ Fuel 2000;14:150–9.

[15] Helble JJ, Srinivasachar S, Boni AA. Factors influencing the transformation of minerals during pulverized coal combustion. Prog Energ Combust Sci 1990;16:267–79.

[16] Chin PP, Ding J, Yi JB, Liu BH. Synthesis of FeS_2 and FeS nanoparticles by high-energy mechanical milling and mechanochemical processing. J Alloy Compd 2005;390:255–60.

[17] Fegley Jr B, Lodders K, Treiman AH, Klingelhöfer G. The rate of pyrite decomposition on the surface of Venus. ICARUS 2000;115:159–80.

[18] Hong Y, Fegley Jr B. The sulfur vapor pressure over pyrite on the surface of Venus planet. Space Sci 1998;45(6/7):683–90.

[19] Subasinghe ND, Akolekar DB, Bhargava SK. Study of mineral reactions of oil shale under different environmental conditions using in-situ hot-stage XRD analyses. Dev Chem Eng Miner Process 2006;14(1–2):277–86.

[20] Oberthür T, Cabri LJ, Weiser TW, McMahon G, Müller P. Pt, Pd and other trace elements in sulfides of the main sulfide zone, great dyke, Zimbabwe: a reconnaissance study. The Can Mineral 1997;35:597–609.

[21] Hurst HJ, Levy JH, Warne SStJ. The application of variable atmosphere thermomagnetometry to the thermal decomposition of pyrite. React Solid 1990;8:159–68.

[22] Hu H, Chen Q, Yin Z, Zhang P. Thermal behaviors of mechanically activated pyrites by thermogravimetry (TG). Thermochim Acta 2003;398:233–40.

[23] Aylmore MG, Lincoln FJ. Mechanochemical milling-induced reactions between gases and sulphide minerals: II. Reactions of CO_2 with arsenopyrite, pyrrhotite and pyrite. J Alloy Compd 2001;314:103–13.

[24] Aylmore MG, Lincoln FJ. Mechanochemical milling-induced reactions between gases and sulfide minerals I. Reactions of SO_2 with arsenopyrite, pyrrhotite and pyrite. J Alloy Compd 2000;309:61–74.

[25] Eymery JP, Ylli F. Study of a mechanochemical transformation in iron pyrite. J Alloy Compd 2000;298:306–9.

[26] Hong Y, Fegley B. The kinetics and mechanism of pyrite thermal decomposition. Ber Bunsen Phys Chem 1997;101:1870–81.

[27] Dunn JG, De GC, O'Connor BH. The effect of experimental variables on the mechanism of the oxidation of pyrite: part 1. Oxidation of particles less than 45 μm in size. Thermochim Acta 1989;145:115–30.

[28] Dunn JG, De GC, O'Connor BH. The effect of experimental variables on the mechanism of the oxidation of pyrite: part 2. Oxidation of particles of size 90–125 μm. Thermochim Acta 1989;155:135–49.